THE SMALL-SIGNAL ac RESPONSE OF $La_{1-x}Ba_xF_{3-x}$ SOLID SOLUTIONS

A. ROOS, D.R. FRANCESCHETTI[‡] and J. SCHOONMAN

Solid State Department, Physics Laboratory, State University,
P.O. Box 80.000, 3508 TA Utrecht, The Netherlands

The small-signal ac response of single crystals of $La_{1-x}Ba_xF_{3-x}$ $(0 \leqslant x \leqslant 0.104)$ with ionically blocking electrodes has been measured in the frequency range 10^{-2} to 10^5 Hz, and for temperatures from 293 to 1300 K. At low and moderate temperatures the ac bulk response can be modeled with a Debye circuit. The circuit parameters do not have the temperature dependence associated with dipolar reorientation but rather the opposite, as is characteristic of the behavior of free charge carriers. We have developed a model, in which the theoretically expected dependence of the circuit parameters is concordant to the behavior found experimentally. Thermally stimulated depolarization current (TSDC) spectra exhibit five dielectric relaxation peaks, in addition to a space-charge peak. Two peaks have been analyzed in detail. The reorientation enthalpies are concordant with the conduction activation enthalpies.

La réponse signal-faible par courant alternatif de monocrystaux du type $La_{1-x}Ba_xF_{3-x}$ $(0 \leqslant x \leqslant 0.104)$ avec des électrodes de blocage des ions a été mesurée dans le domaine de fréquence 10^{-2} à 10^5 Hz, et pour des températures entre 293 et 1300 K. A des températures basses et modérées la réponse du volume par courant alternatif peut être représenté à l'aide du circuit Debye. Les paramètres du circuit ne montrent pas la dépendance de température associée à la réorientation dipolaire mais plutôt l'opposé, ce qui est caractéristique du comportement des porteurs de charge libre. Nous avons développé un modèle où la dépendance attendu théoriquement des paramètres du circuit s'accorde avec le comportement trouvé en expériment. Thermally stimulated depolarization current (TSDC) spectres montrent cinq pics de relaxation diélectrique et en plus un pic de charge d'espace. Deux pics ont été analysés en détail. Les enthalpies de réorientation s'accordent avec les enthalpies de l'activation de la conduction.

1. Introduction

LaF₃ and the solid solutions $La_{1-x}Ba_xF_{3-x}$ adopt the structure of the mineral tysonite (a lanthanum cerium fluoride). At present there is wide-spread interest in the electrical properties of LaF₃ and tysonite (LaF₃)-type solid solutions which are candidates for use in solid state batteries, gas sensors, and ion selective electrodes. The conductivity properties of tysonite materials are rather complex and in some respects poorly understood. The dominant disorder is believed to be of the Schottky type, with the cation vacancies essentially immobile, so that the ionic current is carried by the anion vacancies alone [1]. Usually one considers two different types of anion site in the lattice in the ratio 2 : 1. Anisotropic fluoride ion

‡ On leave from Physics Department, Memphis State University, Memphis, Tennessee, USA.

conductivity has been observed for undoped LaF₃, with $\sigma(\|c \text{ axis}) > \sigma(\perp c \text{ axis})$ [2].

The reactivity of LaF₃ towards oxygen and water vapour appears to interfere strongly in the experimental characterization of the ionic transport. Due to the formation of oxygen-rich surface layers, frequency-dependent effects have been observed. Such layers even tend to mask the intrinsic conductivity region [3].

In order to shed more light upon the modes of conduction, we have studied diffusive and localized motions in single crystals of $La_{1-x}Ba_xF_{3-x} (0 \leqslant x \leqslant 0.104)$. For diffusive motions the small-signal ac response of cells with LaF₃ or a solid solution and ionically blocking electrodes, has been measured. Localized motions in LaF₃ and the solid solutions have been studied using thermal depolarization techniques (TSDC).

2. Experimental aspects

Single crystals of $La_{1-x}Ba_xF_{3-x}(0 \leqslant x \leqslant 0.104)$ were grown by means of a modified Stockbarger crystal growth method, using a RF heater. All crystals appeared to be single-phase with the LaF_3 ($P\bar{3}c1$) structure.

The admittance/impedance data were recorded for temperatures from 293 to 1300 K in the frequency range 10^{-2} to 10^5 Hz, using a frequency response analyser (Solartron 1174). As electrode contact material a platinum paste (6082, Hanovia) was employed. Further we used as ambient dry, purified N_2 gas. The ambient gas is purified with two BTS catalyst traps and two molecular sieve traps. The experimental data were fitted to an equivalent circuit with a computer program, which employs the gradient method of Fletcher and Powell [4].

The TSDC measurements were performed using a cryostat in which temperatures from 4 K to 400 K could be realized. An ambient of dry He gas was maintained in the cryostat. Linear heating rates were achieved using a digital temperature controller with PID control, and a linearized sweep unit. A computer program has been employed to analyse the localized motions. The analysis was obtained by using the Marquardt method, and provides best values for the characteristic relaxation time τ_0, the average activation energy E_0, the width of a gaussian energy distribution σ, and the number of dipoles N_d [5].

3. Results

3.1. Diffusive motions

Fig. 1 presents the bulk electrolyte conductivity of pure LaF_3 as reported in the literature [2]. Up to about 420 K the conductivity of single crystals is slightly anisotropic ($\sigma(\|) > \sigma(\perp)$). The data in fig. 2 reveal the bulk electrolyte conductivity of pure LaF_3 and of $La_{0.896}Ba_{.104}F_{2.896}$. The bulk conductivity of $La_{0.896}Ba_{0.104}F_{2.896}$ is not anisotropic. For solid solutions with smaller solute contents the conductivity is slightly anisotropic. The intrinsic point defects in LaF_3 are assumed to be thermally generated according to a Schottky mechanism $0 \rightleftharpoons V'''_{La} + 3V_F^{\cdot}$. Here the Kröger-Vink defect notation is used.
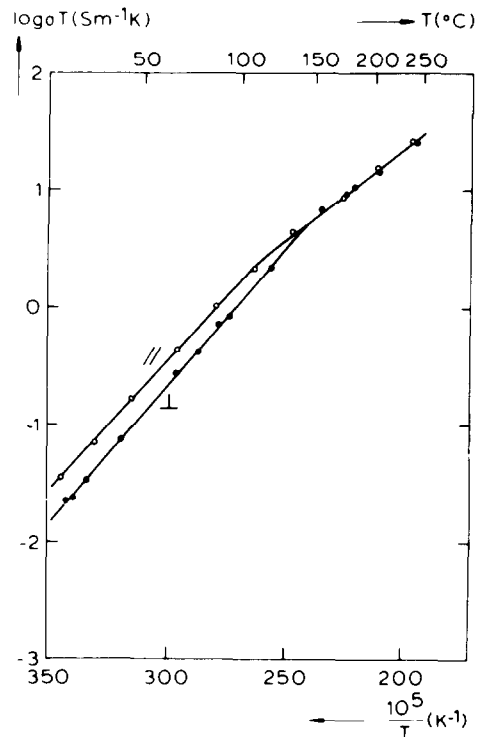

Fig. 1. Bulk electrolyte conductivity of pure LaF_3 ($\perp$ and $\|c$ axis).
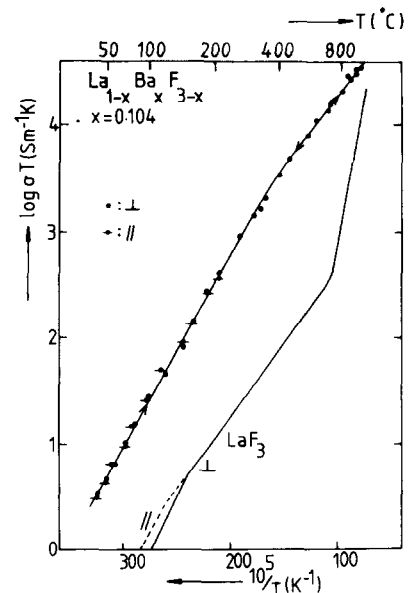

Fig. 2. The bulk electrolyte conductivity of pure LaF_3 and of $La_{1-x}Ba_xF_{3-x}$, $x = 0.104$. The dots represent the solid solution $x = 0.104$; the solid line represents pure LaF_3.
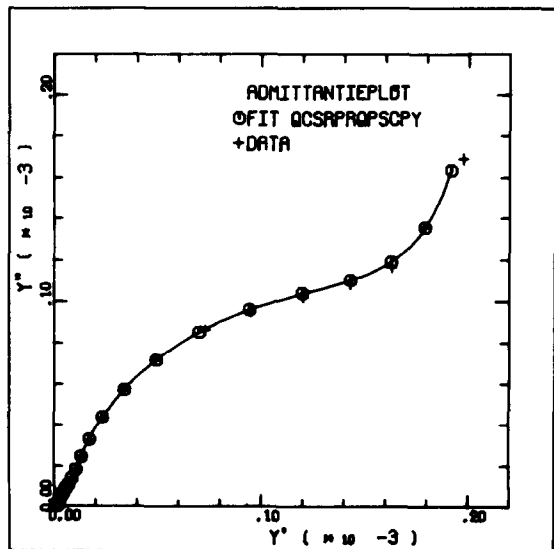
Fig. 3. Admittance spectrum of $La_{0.896}Ba_{0.104}F_{2.896}$ $\perp c$ axis. $T = 325$ K. Frequency range: 3 Hz to 100 kHz.

The fluoride ion vacancies constitute the mobile species. The high-temperature bulk conductivity data of pure LaF_3 lead to the values 0.46 eV and 0.26 eV [migration enthalpies $\Delta H_m(\perp c$ axis)] and 0.84 eV (intrinsic conductivity enthalpy), and hence to the

value 2.32 eV for the Schottky-disorder formation enthalpy. The conductivity data of the solid solutions indicate that the deficiency of anions is not accommodated by the creation of specific vacant anion sites.

We have analyzed the small-signal ac response with a non-linear least-squares fitting procedure, that has been employed to fit the complex data to several equivalent circuits. The data can be fit to high accuracy (relative standard deviations $\approx 1\%$) to a circuit, which includes the Debye circuit segment usually associated with dipolar relaxation. A typical example of a measured and calculated admittance spectrum is given in fig. 3. The concomitant impedance spectrum provides details of the low-frequency region, and is given in fig. 4. The full circuit is presented in fig. 5. The computer program accepts the circuit in the form QCSRPRQPSCPY, where S and P denote series and parallel, respectively, while Y indicates that experimental admittance data have been fitted. It should be noted that the circuit used to fit the data did not include the interfacial capacitance C_2. A detailed analysis of the interfacial phenomena is beyond the scope of this paper, and it will be reported elsewhere.

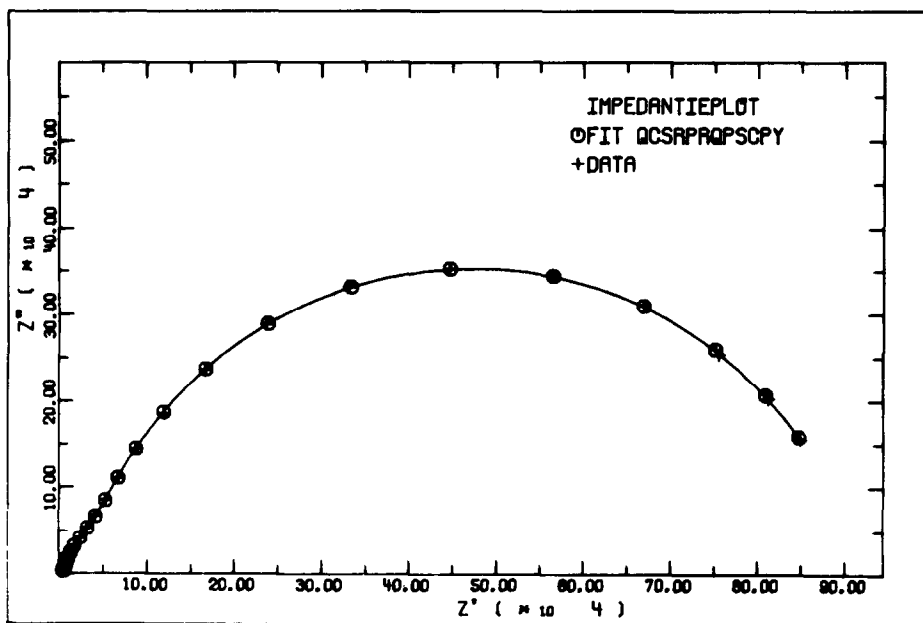The circuit elements Q_1 and C_1 have the following temperature behavior: the capacitance (C_1) is increas-

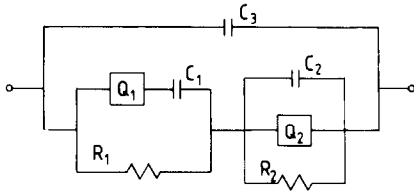Fig. 4. Concomitant impedance spectrum of $La_{0.896}Ba_{0.104}F_{2.896}$, $\perp c$ axis.

Fig. 5. The general equivalent circuit to which data have been fit to high accuracy. Left part: the Debye circuit segment (QCSRP). Right part: the interface circuit segment (QRPCP). Constant phase angle (CPA): $Q_j = k_j(i\omega)^{-\alpha_j}$.

ing with temperature and the series CPA (Q_1) decreasing. Furthermore, α_1 is practically zero indicating the resistive nature of Q_1. Thus these circuit elements do not have the temperature dependence associated with dipolar reorientations, but rather the opposite, as is characteristic of the behavior of free charge carriers.

3.2. Localized motions

The TSDC spectra reveal several relaxations, and a peak due to relaxation of macroscopic space charge, which occasionally masks one dipolar relaxation. This is due to the fact that the temperature of the maximum of the space-charge peak decreases with increasing conductivity. A computer program has been used to analyse the TSDC spectra. The monoenergetic theory for thermal depolarization currents is based on the existence of noninteracting dipoles, and these dipoles reorient with a unique characteristic relaxation time. The experimental spectra revealed peak broadening effects. To account for this peak broadening, the reorientation energy is assumed to have a distribution of width σ around a mean value E_0, due to dipole–dipole interactions. Following van Weperen et al. [6] we have assumed a gaussian distribution of width σ. This then leads to the following TSDC-formula:

$$I(T) = \frac{C}{\tau_0 \sigma \sqrt{2\pi}} \int_{E_0-5\sigma}^{E_0+5\sigma} e^{-E/kT} \exp\left[-\frac{(E-E_0)^2}{2\sigma^2} \right]$$

$$\times \exp\left[-\frac{1}{B\tau_0} \int_0^T e^{-E/kT'}\, dT' \right] dE, \qquad (1)$$

where τ_0 denotes the characteristic relaxation time, C

is a constant (wherein the number of dipoles), and B the heating rate. k and T have their usual meaning. Fig. 6 presents a best fit by this four-parameter TSDC formula. Two relaxation peaks can be fitted with high accuracy, indicating their dipolar nature. The values for E_0 are 0.30 and 0.50 eV, respectively. The number of dipoles involved appeared to be much smaller than the value of x in the deliberately doped solid solution. The dipoles in the nominally pure LaF_3 may be ascribed to oxide–vacancy associates. The relaxation parameters are gathered in table 1.

4. Discussion

At room temperature the anisotropy factor of LaF_3 is about 2. This factor decreases upon increasing the temperature. In general, two types of fluoride ion site (F_1 and $F_2 = F_3$) have been considered in the description of diffusive motion. Powder neutron diffraction data obtained by Cheetham [7] reveal that the dopant BaF_2 generates vacant F_1 sites, table 2.

According to recent structure investigations of pure LaF_3 by Maximov and Schulz [9], the F_3 sites show positional disorder. Furthermore, the main diffusion path seems to run along the c axis. This is in line with the present observation that the conductivity along the c axis exceeds that perpendicular to the c axis. In comparison with pure LaF_3 the conductivity anisotropy of the solid solutions does not change substantially. For high solute contents the anisotropy disappears. Therefore, the present conductivity data do not point to a preferential site for the charge compensating anion vacancy.

The temperature dependence of the extrinsic ionic conductivity of LaF_3 (figs. 1 and 2) reveals a knee, suggesting a classical change-over from a dissociation mode to a free-defect conduction mode. However, the temperature dependence of the bulk circuit elements Q_1 and C_1 (fig. 5) does indicate that a dipole dissociation model cannot, by itself, account for the observed knee, because Q_1 should increase and C_1 decrease with increasing temperature. This analysis points to a model, in which the fluoride ions interchange easily among different types of anion site in the tysonite structure.

The existence of three different types of anion site indicates that in general, the anion conductivity of the
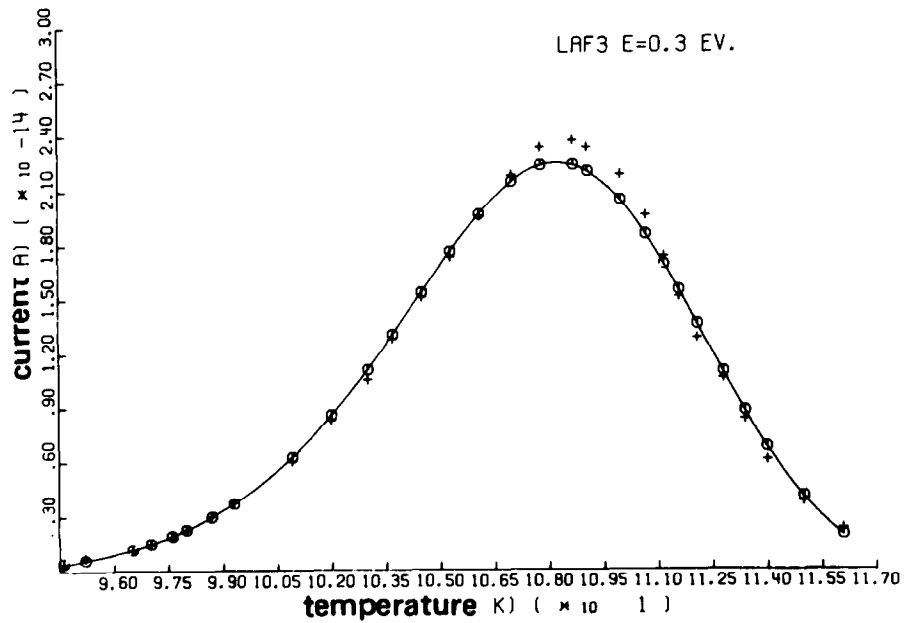
Fig. 6. Experimental points and the best fit by a four-parameter TSDC formula with energy distribution. $E_0 = 0.30$ eV, $\tau_0 = 2.5 \times 10^{-12}$ s^{-1}.

Table 1
Relaxation parameters for LaF$_3$ and La$_{1-x}$Ba$_x$F$_{3-x}$

	$T_m(K)$	τ_0 (s^{-1})	E_0 (eV)	σ(eV)	x_m(m/o)[a]	x_w(m/o)[b]
1	20.3	0.34×10^{-11}	0.01	0.012	—	—
2	45.5	0.11×10^{-8}	0.15	0.038	—	—
3	57.7	0.18×10^{-9}	0.11	0.27	—	—
4	114.3	0.25×10^{-11}	0.30	0.56×10^{-2}	0.04	0.0
5	152.8	0.62×10^{-12}	0.50	0.49×10^{-2}	0.01	2.73

[a] Relative amount of dipoles present.
[b] Relative amount of Ba^{2+} ions present.

Table 2
Atomic coordinates and fluorine occupancy numbers

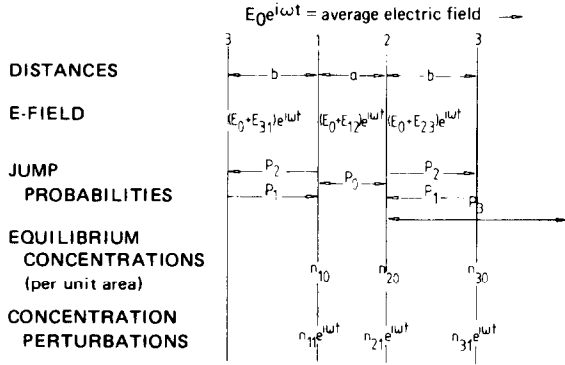|	Tysonite structure P$\bar{3}$c1				
	atomic coordinates			occupancy numbers	
	x	y	z	LaF$_3$	La$_{1-x}$Ba$_x$F$_{3-x}$
La	0.661	0	1/4		
F$_1$	0.3667	0.0540	0.0824	2.0	1.93
F$_2$	1/3	2/3	0.1855	0.67	0.66
F$_3$	0	0	1/4	0.33	0.35

Fig.7. Schematic drawing of the exchange model for anion vacancies in LaF_3. Equilibrium conditions: $n_{10} = n_{20}$, $P_2 n_{10} = P_1 n_{30}$. Electric field: $E_{12} - E_{31} = 4\pi e n_{11}/\varepsilon$, $E_{23} - E_{12} = 4\pi e n_{21}/\varepsilon$, $E_{31} - E_{23} = 4\pi e n_{31}/\varepsilon$. Bulk electroneutrality: $n_{11} + n_{21} + n_{31} = 0$.
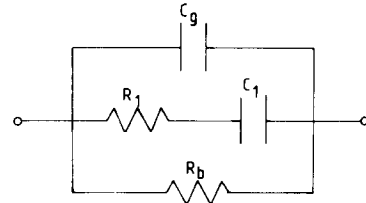

Fig. 8. The theoretical circuit, representing the ac bulk response.

$$R_1 = \frac{lkT}{e^2 c_0}$$

$$\times \frac{(P_2 + 2P_3 + 2P_0)(2 + P_2/P_1)}{\{(P_2 + 2P_3)[2b^2(P_2 + 2P_3) - 4abP_0] + 2P_0^2 a^2\}}, \tag{3}$$

$$C_1 = \frac{e^2 c_0}{lkT}$$

$$\times \frac{\{(P_2 + 2P_3)[2b^2(P_2 + 2P_3) - 4abP_0] + 2P_0^2 a^2\}}{(2 + P_2/P_1 + ab/L_{Dl}^2)(P_2 + 2P_3 + 2P_0)^2}, \tag{4}$$

$$R_b = \frac{lkT}{e^2 c_0} \frac{(P_2 + 2P_3 + 2P_0)(2 + P_2/P_1)}{P_0(P_2 + 2P_3)(a + 2b)^2}, \tag{5}$$

where l is the thickness of the sample, c_0 is the concentration of anion vacancies, a and b are the distances indicated in fig. 7 and L_{Dl} is the one-mobile Debye length for the anion vacancies.

Since c_0 increases exponentially with temperature in the intrinsic region, this model predicts that R_1 will decrease and C_1 increase with temperature, in contrast to the behavior to be expected from the presence of bound dipolar complexes. The precise temperature dependence of the parameters will be determined by the preexponential factors and activation enthalpies of the jump probabilities $P_0, \ldots, P_3$. Preliminary studies indicate that $(1/R_b T)$ versus $(1/T)$ plots calculated from this model can, to some extent, mimic the transition from association to free conduction.

If we assume $P_2 = 0$ and $P_1 = P_2$ then the bulk conductance $G_b(R_b^{-1})$ is proportional to $P_0 P_3/(P_0 + P_3)$. Fig. 9 presents two possibilities for the theoretical bulk electrolyte conductivity, indicating that this model can explain indeed a knee in the temperature dependence of the extrinsic conductivity (fig. 1).

material cannot be interpreted in terms of a single thermally activated jump probability, as is the case for simpler materials. Even if one treats the F_2 and F_3 sites as equivalent, at least three different kinds of anion jump are possible: $F_1 - F_1$, $F_1 - F_2$ and $F_2 - F_2$. A model has now been developed [8] for the small-signal bulk ac response of tysonite type materials which does lead to a Debye-type of equivalent circuit without the assumed presence of dipolar complexes.

In examining a model of the tysonite structure one finds that in the direction of the c axis, and in the direction of the bisector of the a and b axes, the lattice planes occur in the pattern AABAAB, where "A" denotes a plane containing only F_1 type fluoride sites and "B" denotes a plane containing F_2 and F_3 type sites, here treated as equivalent. This situation is indicated schematically in fig. 7, where zero-field transition probabilities P_0, P_1, P_2 and P_3 are indicated for the different possible jumps of anion vacancies between neighboring lattice planes.

The bulk small-signal ac behavior of LaF_3 has been examined theoretically, using the standard thermally activated form for the jump probabilities. The analysis leads directly to the Debye-type of equivalent circuit (fig. 8) with the circuit parameters given (per unit area) by
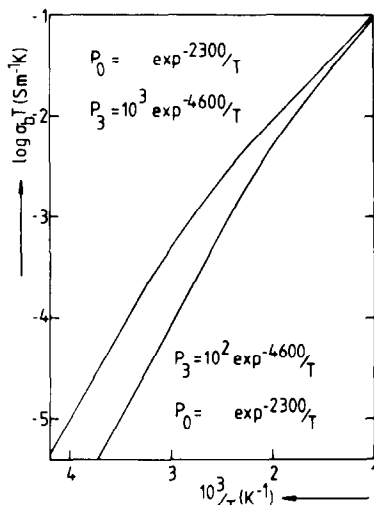
$$C_g = \varepsilon/4\pi l, \tag{2}$$

Fig. 9. Theoretical bulk electrolyte conductivity.

The TSDC spectra reveal in addition to the space-charge peak (reflecting ionic conductivity) five relaxations. Two of these relaxations have been analyzed in detail. The reorientation enthalpies agree with the extrinsic conduction activation enthalpies for fluoride ion vacancies, i.e. $\Delta H_\sigma(V_F^-) = 0.46$ eV and 0.26 eV; $\Delta H_R(E_0) = 0.50$ eV and 0.30 eV.

This is to be expected for dipoles containing fluoride ion vacancies. For the solid solutions the dipoles are of the type $(Ba_{La}V_F)^\times$. For the nominally pure material the aliovalent impurity is unknown. An obvious impurity in these fluoride systems is oxygen, the dipole then being of the type $(O_FV_F)^\times$. The present results indicate that the dipolar effects are hidden in the conduction phenomena.

Acknowledgement

References

[1] Gmelin Handbuch der Anorganischen Chemie, Seltenerdelemente, Teil C3, Sc, Y, La und Lanthanide, 8th Ed. (Springer, Berlin, 1976) pp. 50, 51, 98–100, 158, 159.

[2] J. Schoonman, G. Oversluizen and K.E.D. Wapenaar, Solid State Ionics 1 (1980) 211.

[3] A.V. Chadwick, D.S. Hope, G. Jaroszkiewicz and J.H. Strange, in: Fast ion transport in solids, eds. P. Vashishta, J.N. Mundy and G.K. Shenoy (North-Holland, Amsterdam, 1979) pp. 683–686.

[4] R. Fletcher and M.J.D. Powell, Computer J. 6 (1963) 163.

[5] D.W. Marquardt, J. Siam. 11 (1963).

[6] W. van Weperen, B.P.M. Lenting, E.J. Bijvank and H.W. den Hartog, Phys. Rev. B16 (1977) 2953.

[7] A.K. Cheetham, University of Oxford, unpublished results.

[8] D.R. Franceschetti and P.C. Shipe, Solid State Ionics 11, (1984) 285.

[9] H. Schulz, MPI-Stuttgart, private communication.